CORTEX

Research and Innovation Action (RIA)

This project has received funding from the European Union's Horizon 2020 research and innovation programme under grant agreement No 754316.

Start date : 2017-09-01 Duration : 48 Months
http://cortex-h2020.eu

Results of the sensitivity analyses

Authors : Mrs. Soobeen YUM (TU München), Mr. Yann Perin (GRS)

CORTEX - Contract Number: 754316

Project officer: Marco Carbini

Document title	Results of the sensitivity analyses
Author(s)	Mrs. Soobeen YUM, Mr. Yann Perin (GRS)
Number of pages	28
Document type	Deliverable
Work Package	WP04
Document number	D4.5
Issued by	TU München
Date of completion	2021-08-15 10:34:46
Dissemination level	Public

Summary

In this report, a series of sensitivity analyses are carried out assuming the oscillation of one fuel assembly (FA) in the Swiss 3-loop pre-Konvoi reactor. In the framework of the CORTEX project, the two-energy groups nuclear data are provided by PSI which were generated for five different core conditions. Among the given five core conditions, three conditions are selected for further analyses to investigate the effects of fuel loading pattern and fuel burnup on the sensitivity of input parameters. The general methodology for the sensitivity analysis is based on the preceded work described in deliverable D1.1 and modified to reflect the reactor type and the event in the current study. The neutron noise is calculated with the noise simulator CORE SIM+ and the sensitivity indices are obtained from 300 data sets. From the analyses with three different core conditions, it is confirmed that with increasing fuel burnup the sensitivity on the 'location of noise source' increases remarkably. This is because at the EOC a steeper static flux gradient exists around the oscillating fuel assembly than at the BOC, and this steeper gradient acts like a weighting factor to the noise source. Different from the fuel burnup condition, the fuel loading pattern generates little change and the 'location of noise source' is maintained as the most influential parameter.

Approval

Date	By
2021-08-16 11:05:52	Mr. Joachim HERB (GRS)
2021-08-17 08:34:43	Pr. Christophe DEMAZIERE (Chalmers)

Table of Contents

Index of Tables

Table of Figures

This project has received funding from the Euratom research and training programme 2014-2018 under the grant agreement no.754316. The content in this report reflects only the views of the authors. The European Commission is not responsible for any use that may be made of the information it contains.

Abbreviations

SA	Sensitivity Analysis
FA	Fuel Assembly
KKG	Kernkraftwerk Gösgen
UO_2	Uranium Oxide
MOX	Mixed Oxide
BOC	Beginning Of Cycle
MOC	Middle Of Cycle
EOC	End Of Cycle
PSI	Paul Scherrer Institute
UC	Uncertainty Characterization
A.P.	Axial Position
R.P.	Radial Position
PCC	Pearson's Correlation Coefficient

Summary

In this report, a series of sensitivity analyses are carried out assuming the oscillation of one fuel assembly (FA) in the Swiss 3-loop pre-Konvoi reactor. In the framework of the CORTEX project, the two-energy groups nuclear data are provided by PSI which were generated for five different core conditions. Among the given five core conditions, three conditions are selected for further analyses to investigate the effects of fuel loading pattern and fuel burnup on the sensitivity of input parameters. The general methodology for the sensitivity analysis is based on the preceded work described in deliverable D1.1 and modified to reflect the reactor type and the event in the current study. The neutron noise is calculated with the noise simulator CORE SIM+ and the sensitivity indices are obtained from 300 data sets. From the analyses with three different core conditions, it is confirmed that with increasing fuel burnup the sensitivity on the 'location of noise source' increases remarkably. This is because at the EOC a steeper static flux gradient exists around the oscillating fuel assembly than at the BOC, and this steeper gradient acts like a weighting factor to the noise source. Different from the fuel burnup condition, the fuel loading pattern generates little change and the 'location of noise source' is maintained as the most influential parameter.

1 Introduction

This report introduces a detailed process of sensitivity analyses (SA) as well as the corresponding results under fuel assembly (FA) oscillating condition in a Swiss 3-loop pre-Konvoi reactor. The noise behaviour is simulated by the noise simulator CORE SIM+ for various core conditions (different fuel burnups and fuel loading patterns). The sensitivity analysis identifies the relative importance of the considered input parameters to the neutron noise at the installed detector locations. Additionally, by the repetition of the identical analysis under different core conditions, the influence of the fuel burnup and the fuel loading pattern on the sensitivity of the input parameters is also investigated.

2 Description of Target Experiments

2.1 Target Reactor

The target reactor considered here is the Gösgen Nuclear Power Plant (officially named 'Kernkraftwerk Gösgen (KKG)'), which is located in the Däniken municipality, in Switzerland. It is operated by the Kernkraftwerk Gösgen-Däniken AG, since the start of its operation in 1979 [1]. The reactor is licensed to operate at a nominal thermal power of 3002 megawatts.

The KKG possesses a pressurized water reactor delivered by German Kraftwerk Union AG. It contains 177 fuel assemblies, while 48 of which are equipped with control elements. Each fuel assembly contains 205 fuel rods, which consist of enriched UO_2 with fissile uranium-235 or MOX fuel elements (uranium-plutonium mixed oxide fuel elements) with a proportion of fissile plutonium. However, MOX fuel has not been used since 2012. Inside each fuel rod, a column of fuel pellets is enclosed in a gas-tight and pressure-resistant-welded Zircaloy cladding tube.

In the context of the CORTEX project, the Paul Scherrer Institute (PSI) provided the necessary core data, which include three-dimensional distribution of the nodal macroscopic cross-sections in two-energy groups and the kinetic parameters of Cycle 39 (MOC and EOC) and Cycle 40 (BOC, MOC and EOC) [2]. Accordingly, the analyses are carried out based on these core conditions.

2.2 Target Event Inducing the Neutron Flux Oscillation

Experimental reactors, such as AKR-2 or CROCUS [3, 4], have their own dedicated experimental facilities, which enables us to plan the relevant noise experiments within their capabilities. However, in power plants during normal operation no neutron noise experiments can be performed to get measurements for perturbations which can be precisely reproduced by simulations. Therefore, an event which induces the neutron noise has been chosen based on the analyses performed so far and which are reported in deliverable D4.4.

The relevant event is a 'vibration of 1 fuel assembly', where the size of fuel assembly corresponds to $21.56\ cm \times 21.56\ cm \times 358\ cm$ and the oscillating fuel assembly is located $53.9\ cm$ away from the core center as shown in Figure 1.

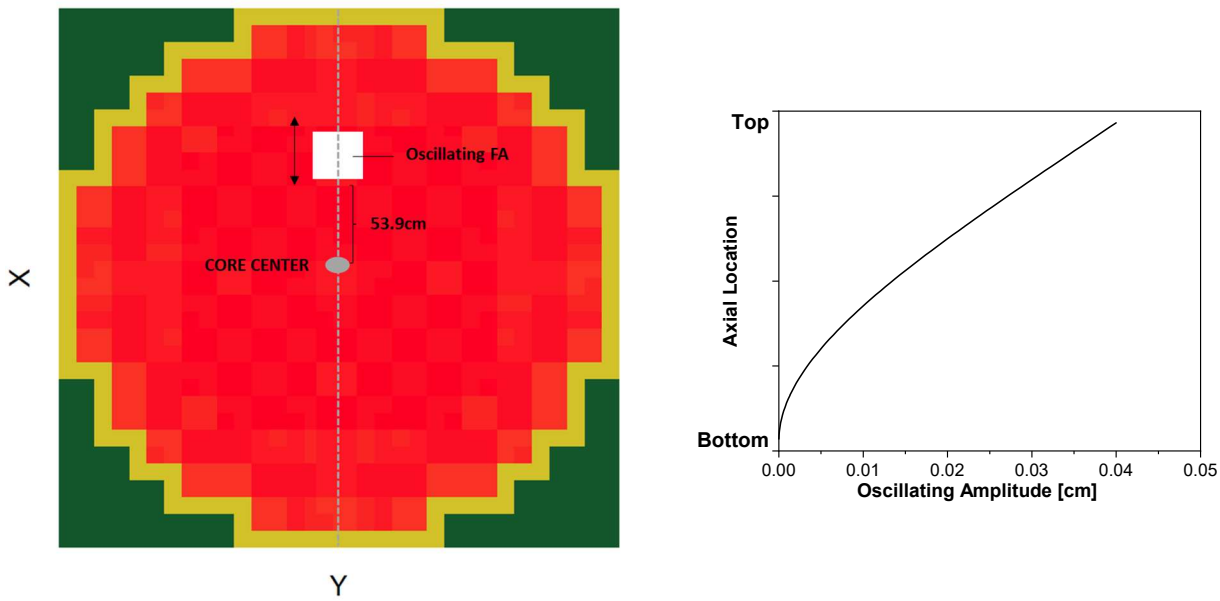

Figure 1: The location of vibrating fuel assembly in core radial map (left) and the oscillating amplitude with height (right)

It is assumed that the fuel assembly oscillates following the cantilevered beam mode whose oscillating amplitude increases along the axial height as described on the right side in Figure 1 [5]. Additionally, the oscillating frequency of the fuel assembly is presumed as 1 Hz.

2.3 Neutron Noise Calculation

The noise behaviour under this condition is simulated with CORE SIM+ [6], a neutron noise simulator based on the two-energy group kinetic neutron diffusion equations and capitalizes the former CORE SIM tool [7]. The core is modelled with a three-dimensional mesh of $76 \times 51 \times 102$ cells, in the $x-$, $y-$ and $z-$ directions of the core, respectively. The area around the neutron noise source is modelled with the fine meshes with the size of $4.3\ mm$, whereas the rest area is modelled with coarser meshes, whose sizes are varying between $3\ cm$ and $10\ cm$, depending on the region of interest. Figure 2 shows the modelled reactor core at the axial mid-point.

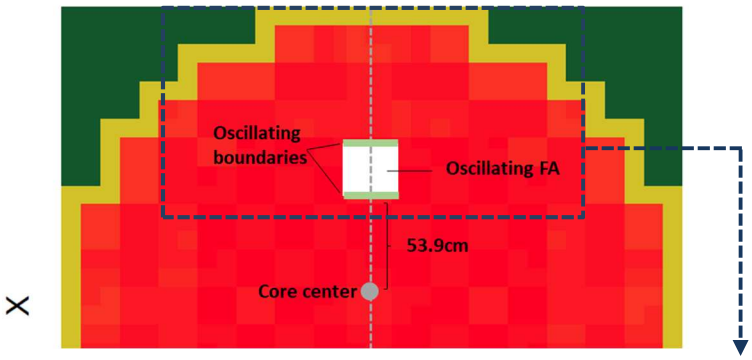

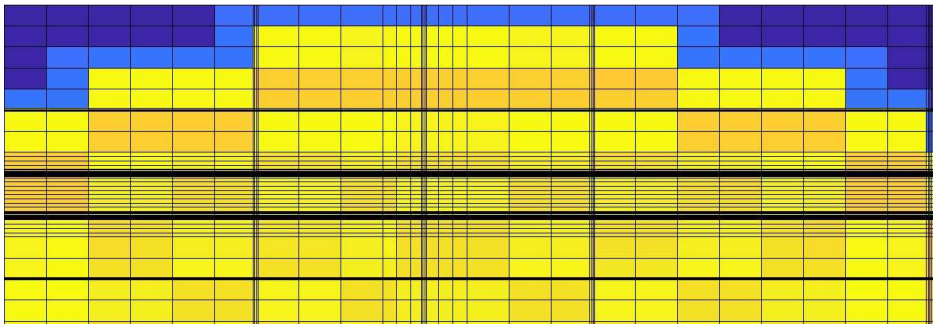

Figure 2: Modelled noise source in CORE SIM+ (upper) and the area around oscillating fuel assembly modelled with fine meshes (lower)

The two green lines at the boundaries of oscillating fuel assembly represent the location where the noise sources are assigned for the noise simulation using CORE SIM+. The lower picture of Figure 2 focuses on the meshes modelled around oscillating fuel assembly, showing the finer meshes at the oscillating boundaries compared to the rest area.

3 Preparation for the Analysis

3.1 Process of Analysis

The framework of the analysis process regarding the uncertainty characterization (UC) and the noise simulation is based on the methodology reported in the deliverable D1.1, applied to the CROCUS reactor in the context of the CORTEX project [8]. The main changes compared to the previous work are:

1) This study only focuses on sensitivity analysis and excludes uncertainty propagation since the validation of the neutron noise simulator is not a main concern in this work.
2) The step for the generation of the nuclear data by using the Monte-Carlo particle transport code (Serpent) is removed as the relevant nuclear data are directly provided by PSI.

The workflow chart reflecting the modification above is depicted in Figure 3. The selected input parameters are considered in both steady-state and dynamic calculations using CORE SIM+ as follows. Based on the selected core condition, the two energy-group cross-sections and the core kinetic parameters are determined, and their corresponding uncertainties are generated. Then N steady-state calculations are carried out with CORE SIM+, resulting in N static solutions. The obtained static fluxes are then combined with noise sources which are perturbed within the uncertainty ranges and used as inputs for noise calculations. The further sensitivity analysis is carried out by using the obtained N neutron noise solutions from CORE SIM+ calculation. The output from the simulation is a complex quantity, therefore, a relevant post-process is carried out to derive the amplitude and the phase of neutron noise from the original output. However, for the sake of the applicability, the focus is limited to the thermal neutron noise since the installed detectors in the reactor do not detect the oscillations of the fast neutron flux.

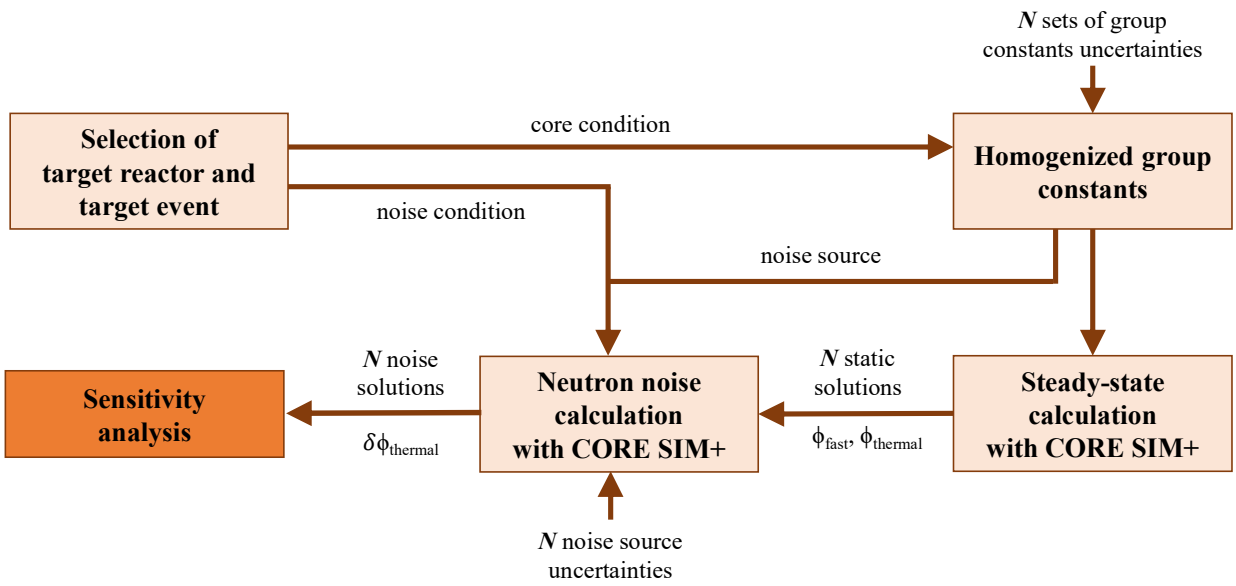

Figure 3: Workflow chart for the sensitivity analysis

3.2 Listing Input Parameters

A total of 13 input parameters for the target reactor and transient are investigated based on expert judgement as summarized in Table 1. The oscillating amplitude and frequency are designed to be perturbed with a standard deviation of 5% around their nominal values.

Table 1: The information of selected uncertain parameters

No.	Parameter	Distribution	Unit	Mean	Standard deviation[1] (Lower/Upper limit[2])
1~7	Nuclear data uncertainties[3]				
8	Oscillating amplitude	Normal	cm	Inherent oscillating curve in Figure 1	5%
9	Oscillating frequency	Normal	Hz	1	0.05
10	Location of noise source	Uniform	Mesh	Ideal oscillating boundary	-1/+1[4]
11	Detecting location (x-axis)	Uniform	Mesh	Ideal oscillating boundary	-1/+1[4]
12	Detecting location (y-axis)	Uniform	Mesh	Ideal oscillating boundary	-1/+1[4]
13	Detecting location (z-axis)	Uniform	Mesh	Ideal oscillating boundary	-1/+1[4]

1: This column shows the standard deviation in case of having normal distribution.

2: This column shows the value of lower and upper limit in case of having uniform distribution.

3: Nuclear data uncertainties are treated in a distinct manner as they are propagated to seven parameters: five macroscopic cross-sections as well as two diffusion coefficients. Detailed information regarding the uncertainty propagation process is provided in a following paragraph.

4: -1/+1 correspond to -0.43/+0.43 cm.

The Swiss 3-loop pre-Konvoi reactor KKG has a total of 36 in-core detectors. They are installed in 6 different axial positions and each axial position consists of 6 detectors in different radial positions (see Figure 4 [9]). The 36 detecting locations are perturbed between -1 mesh and +1 mesh from the ideal locations, in the $x-$, $y-$ and $z-$ directions of the core.

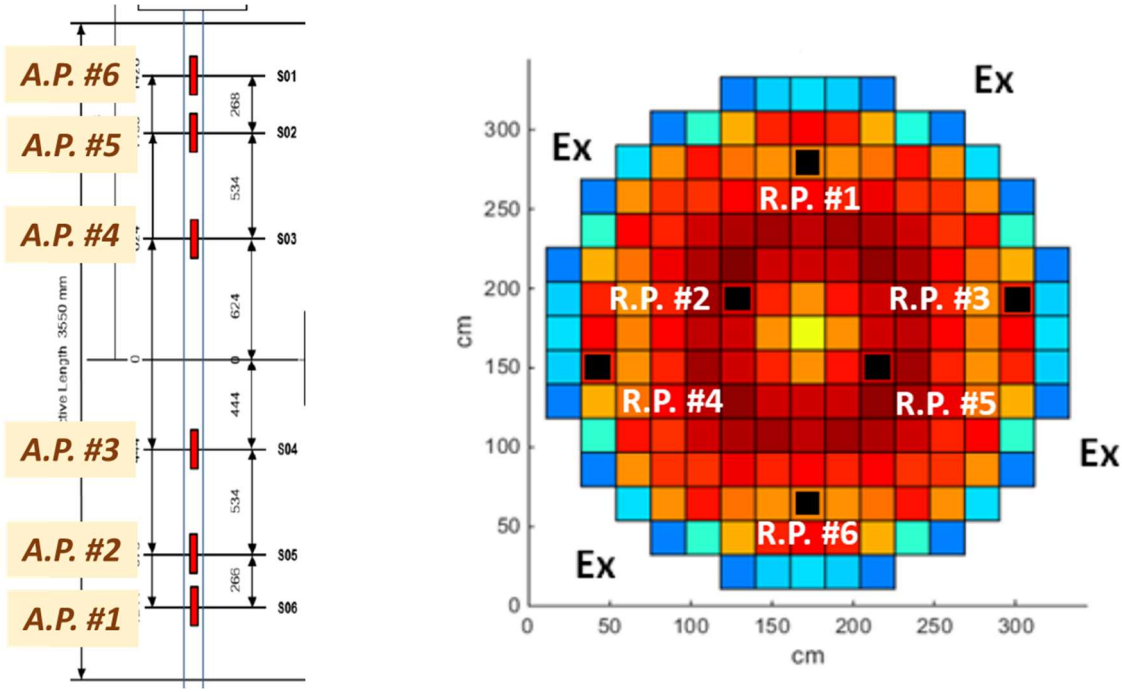

Figure 4: The installed locations of in-core detectors ('A.P.' and 'R.P.' denote 'Axial position' and 'Radial position', respectively.)

The group constants uncertainties are generated from the sampling of nuclear data. This sampling requires an extra explanation since it involves many correlated inputs. SAMPLER is a stochastic uncertainty quantification tool part of the SCALE package (as opposed to TSUNAMI which offers a perturbation theory approach) [10]. It allows the quantification of uncertainty due to uncertainties in:

- neutron cross-sections
- fission yield and decay data
- any user input parameter of a SCALE component.

This study only considers the neutron cross section uncertainty. This is achieved by using the master sample file included in SCALE. This master file contains 1000 samples of perturbation factors for all groups and reactions in all materials which have been pre-computed using the Medusa module of the XSUSA program.

The following data can be found in D4.2:

- The fuel loading pattern for cycles 39 and 40.
- The (fresh) fuel assembly description, including the necessary information for the generation of SCALE models.

All SCALE models use thermal-hydraulic conditions representative of core-averaged conditions at Hot Full Power, namely a fuel temperature of 900K and a moderator density of 707 kg/m³.

Since all the fuel assembly types from these two cycles differ only slightly in enrichment, two fuel assembly SCALE models are considered using the minimum and maximum enrichments (4.90% and 5.06%) found in cycles 39 and 40.

No information is available regarding the burnup distribution for either cycle. Therefore, the effect of burnup on the neutron cross section uncertainty is treated by considering fresh fuel and fuel at 30 MWd/tHM.

The test matrix presented in Table 2 gives a representation of which parameter combinations are studied.

Table 2: Test matrix

	Fuel burnup effect	
Enrichment effect	5.06% Enrichment @ 0MWd/t Burnup	5.06% Enrichment @ 30MWd/t Burnup
	4.9% Enrichment @ 0MWd/t Burnup	

Three hundred varied macroscopic cross-sections were generated using SAMPLER for each of the cases presented above. From those 300 samples of macroscopic cross-sections, relative variations from the reference version of the nuclear data libraries are computed and are applied to vary the existing CORE SIM+ cross-section libraries. The standard deviation of ratios between the samples and the reference case is presented in Table 3. The standard deviations remain low (maximum < 0.3%). The resulting sensitivity on the neutron noise phase and amplitude is presented in the following chapters.

Table 3: Perturbation of nuclear data ratios (standard deviation of ratios between 105 samples and nominal case)

	D_{fast}	$D_{thermal}$	$\Sigma_{abs, fast}$	$\Sigma_{abs, thermal}$	$\Sigma_{nufis, fast}$	$\Sigma_{nufis, thermal}$	Σ_{rem}
Case 1 5.06%@0MWd/t	4.35E-04	9.22E-04	4.12E-03	7.07E-04	2.63E-03	1.32E-03	1.16E-03
Case 2 5.06%@30MWd/t	4.85E-04	8.17E-04	4.10E-03	7.73E-04	2.18E-03	2.11E-03	1.50E-03
Case 3 4.9%@0MWd/t	4.37E-04	9.20E-04	4.18E-03	7.02E-04	2.62E-03	1.31E-03	1.16E-03

3.3 Sensitivity Measures

CORE SIM+ solves the dynamic neutron oscillation problem by using the linear theory approximation, thus neglecting the second-order terms in the balance equation for the neutron noise that may induce non-linearities in the solution of the neutronics equations [11]. This simplifies the mathematical complexity and allows us to consider the statistically based approaches for sensitivity analysis, which avoid the need to modify the code to introduce the variation techniques, e.g., regression or correlation-based approaches. Therefore, the Pearson's correlation coefficient (PCC) is selected for sensitivity measures because of its simplicity and ease of use. The PCC is a measure of linear correlation between two sets of data, whose value corresponds to the covariance of two variables, divided by the product of their standard deviations [12, 13]. The PCC (commonly represented by the Greek letter ρ) between two random variables (X, Y) can be defined as follows:

$$\rho_{X,Y} = \frac{cov(X,Y)}{\sigma_X \sigma_Y} \tag{1}$$

where cov is the covariance and σ_X and σ_Y are the standard deviations of X and Y, respectively.

Additionally, a Z test is carried out in order to determine whether the obtained correlation coefficients are statistically significant. With the test, we set a significance level, which is a threshold of probability depending upon which we decide whether we accept or reject our null hypothesis. Following a general guideline, it is taken as 5% and finally the critical value of the coefficient is obtained as 0.11 with a sample size of 300 by using the Z test [14, 15]. This means that, if the absolute value of the calculated PCC based on 300 samples is larger than 0.11, we can regard that the input and output variables are 'correlated' with a 5% probability that this correlation is not true (95% confidence level).

As a last step, the calculated coefficient is squared to represent the 'sensitivity index', which expresses what fraction of the variation of dependent variable is explained by the variation in the independent variable [16].

4 Outcome of the Sensitivity Analyses

To confirm how the core condition affects the sensitivity of input parameters to the neutron noise, three conditions are selected from the viewpoint of fuel loading pattern and fuel burn-up: to check the influence of loading pattern, EOC 39 and EOC 40 are selected, while BOC and EOC in cycle 40 are considered to confirm the fuel burn-up effect. For each core condition, the homogenized nuclear data at the corresponding condition are used as nominal data.

4.1 Setup the Analysis Condition

4.1.1 Convergence Test

A series of convergence tests are performed with varying the number of samples. This test is necessary to find out an optimal sample size which strikes the balance between computational cost and reliability of the calculated sensitivity index. The tests are carried out with different sample sizes between 10 to 500 under the conditions of BOC 40. The sampling of equivalent sample size is repeated for 1000 times using bootstrapping with replacement [17]. For each sample size, the sensitivity indices are calculated for 1000 times between the input parameters and the amplitude of thermal neutron noise. Afterwards, the 2.5th and 97.5th percentile of the 1000 sensitivity indices are identified to build 95% confidence interval. Figure 5 shows the converging trend of two representative sensitivity indices: 'fast ν-fission cross-section' which has relatively small index and 'location of noise source' which has relatively large index at the location of detector 2.

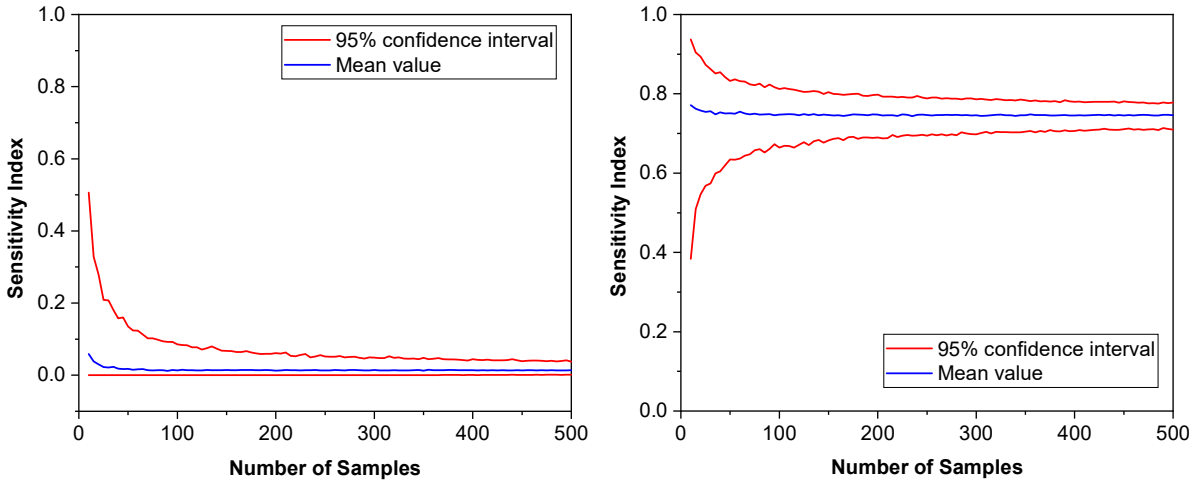

a. Fast ν-fission cross-section b. Location of noise source

Figure 5: Convergence plots of sensitivity indices with 95% confidence interval

The confidence interval decreases as the sample size increases. When the sample size is larger than 300, a difference between the calculated confidence interval (with a sample size larger than 300) and the final estimation with 500 samples becomes smaller than 0.15.

Considering a small difference with the final estimation, further analyses with different core conditions will be carried out using a sample size of 300.

4.1.2 Sensitivity test on nuclear data uncertainty

The reactor core consists of 177 fuel assemblies whose enrichments and burn-up conditions are different from each other. Therefore, to assure the accuracy of the analysis, the nuclear data uncertainties should be calculated by considering the characteristics of individual fuel assemblies. However, this realistic approach increases the computational cost and also complicates the modelling for the noise calculation. For this reason, a simplified approach is introduced by assuming that all fuel assemblies have identical nuclear data uncertainties which are generated for a specific

enrichment and burn-up condition. To study the effect of this simplification, a series of sensitivity analyses are performed with varying the nuclear data uncertainties calculated from three different core condition as introduced in Table 2.

For each case, nuclear data uncertainties are generated for the corresponding core conditions as explained in Section 3.2 and the obtained set of uncertainties is adopted to all fuel assemblies. The three cases of sensitivity analyses are carried out with the BOC 40 set as the nominal core condition. Therefore, the identical homogenized group constants from BOC 40 are used as nominal values for all three cases.

The main concern of the sensitivity analysis is to identify the major contributors to the noise behaviour. Hence, the parameters having relatively large sensitivity indices are used for comparing the results from the three different cases. In this context, the two parameters having the largest sensitivity indices at the installed detector locations are compared between each other: (1) oscillating amplitude and location of noise source for the amplitude of neutron noise, (2) fast absorption cross-section and location of noise source for the phase of neutron noise. Figure 6 compares the sensitivity indices calculated for different neutron noise fluxes, which are obtained from the three different nuclear data uncertainties (corresponding to Cases 1, 2 and 3). Figure 6-a and 6-b show the sensitivity indices between the two aforementioned input parameters and the neutron noise (amplitude and phase) at the installed detector locations. Each comparison consists of 72 points: 36 in-core detectors × 2 input parameters. The x −axis represents the sensitivity indices calculated with the Case 1 condition, while the y −axes show the indices calculated with Case 2 and Case 3 conditions.

From the comparison, it is found that the three different nuclear data uncertainties obtained from three different fuel conditions do not cause significant differences in results, since there is no strong dispersion around the line $y = x$. This comparison shows that an exact reactor model (core condition, assumption of one-homogenized uncertainties for all FAs/different uncertainty for each FA) used to generate the nuclear data uncertainties does not affect the results in a significant manner. Accordingly, further analyses are carried out with a simplified modelling approach that assumes all the fuel assemblies having identical nuclear data uncertainties.

In the following analyses, the uncertainties from Case 1 are used at the BOC 40, while the uncertainties from Case 2 are used at the EOC 39 and 40. These combinations are made to perform the analysis at the specific core condition with the nuclear data uncertainties generated from the burn-up condition mostly similar to the given core condition within the available options in Table 2. Therefore, nuclear data uncertainties generated from ‘lower burn-up condition’ are used at BOC, while the data generated with ‘higher burn-up condition’ are used at EOC. However, as it is confirmed in Figure 6, using different nuclear data uncertainties will not bring any remarkable change in results.

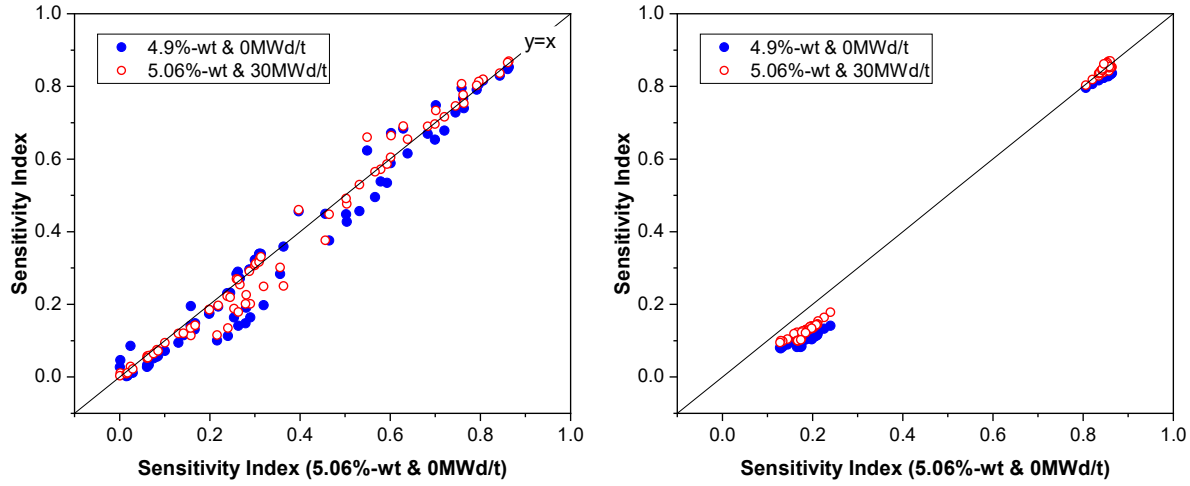

a. Amplitude of thermal neutron noise b. Phase of thermal neutron noise

Figure 6: The comparison of sensitivity indices calculated with different nuclear data uncertainties which are obtained from various fuel condition

4.2 Results

4.2.1 Sensitivity analysis at BOC 40

Figure 7 shows the distribution of the thermal neutron noise in the radial core direction for the unperturbed (nominal) condition.

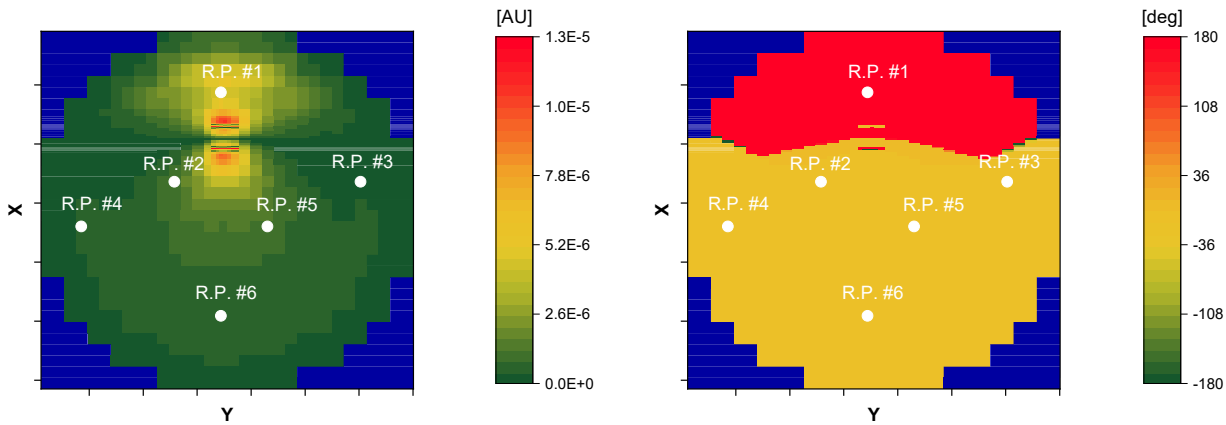

a. Amplitude b. Phase

Figure 7: Thermal neutron noise behaviour at the axial position #3 in BOC 40

To get a better understanding on the noise behaviour at the installed detector locations, correlation matrices for the amplitude and phase of the thermal neutron noise are calculated based on 300 data sets as shown in Figure 8. This correlation information helps us to infer the noise behaviour at the specific detector location by reading the signals from the correlated detectors. Additionally, it enables us to perform the group-wise uncertainty analyses, which simplifies the interpretation process of the calculation results.

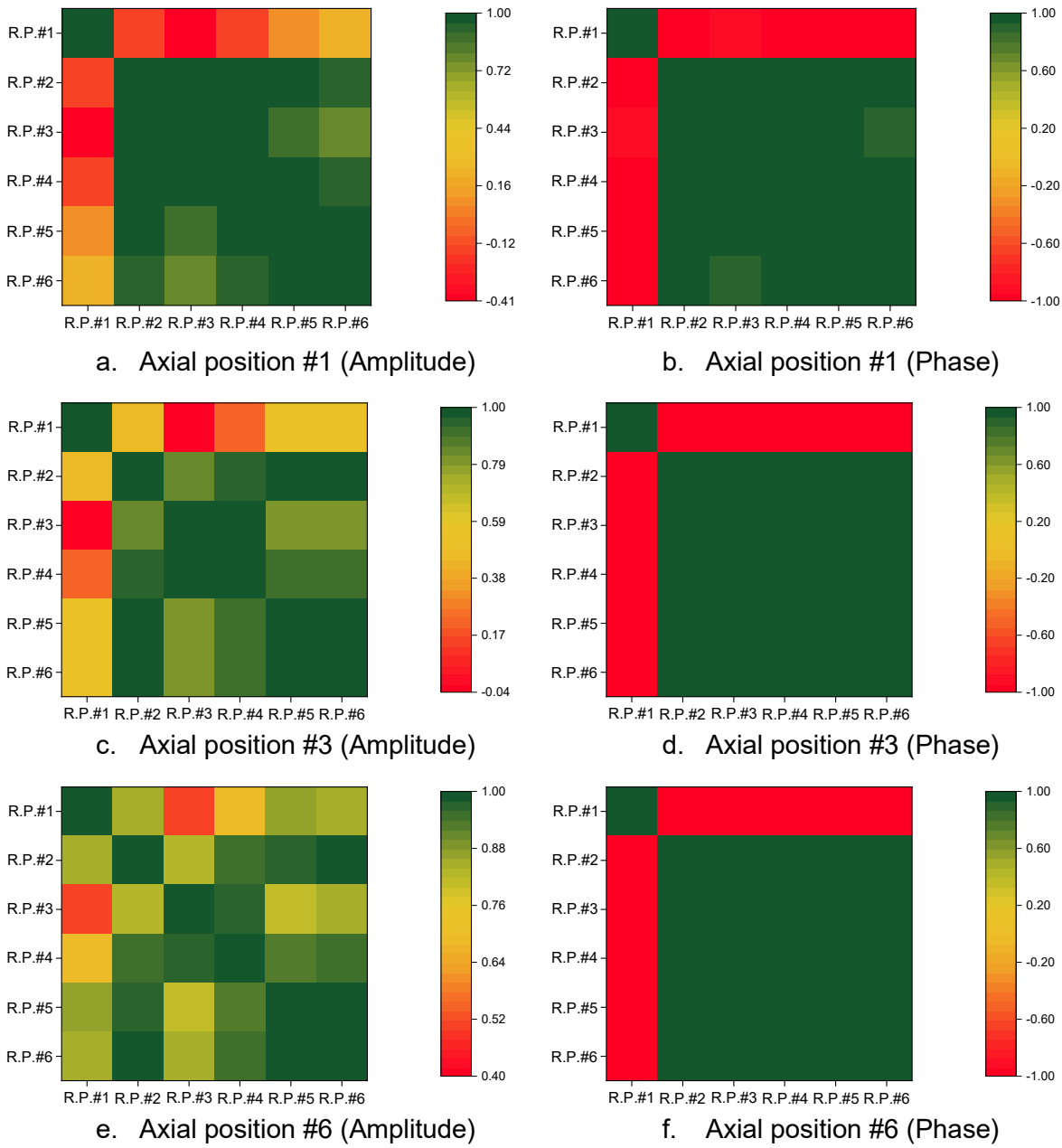

Figure 8: The correlated behaviour among the amplitude and the phase of thermal neutron noise at the detector locations

In case of the amplitude of thermal neutron noise, the value at the radial position #1 shows little correlation with others in all axial positions. The values at the rest five radial positions (R.P #2 ~ R.P #6) are correlated in a similar manner as compared to at the lowest position (Axial position #1). The detectors can be radially subdivided into three groups from the mid-height to the top of the core according to the three different correlations: group 1 consists of the signal at the radial position #1, group 2 consists of the signals at the radial positions #2, #5 and #6, group 3 consists of the signals at the radial positions #3 and #4.

Meanwhile, the phase data show simpler correlations, which are identical in all axial positions. The data at radial positions #2 to #6 have almost perfect positive linear correlations among each other and have perfect negative linear correlations with the value at radial position #1.

Since the correlations exist among the thermal neutron noise at the installed detectors, the uncertainties of the noise (distribution range of the neutron noise) are also expected to show the correlated responses among the detectors. That is, when the signals at two detectors are correlated,

their uncertainties respond in the same direction, either increase or decrease, as the input parameters are perturbed. As a result, the correlated detector signals are expected to have similar sensitivities to the input parameters, which will be investigated in the following sections.

Simplified approach with grouped parameters

To determine the major contributors in macroscopic viewpoints, the entire 13 input parameters listed in Table 1 are grouped into three groups according to the similarities they have in between: (1) group of nuclear data, (2) group of noise source data, (3) group of detecting location. The group of detecting location include the perturbation of the detector location in the $x-$, $y-$ and $z-$ directions. The group of noise source data includes the *oscillating amplitude*, the *oscillating frequency,* and the *location of the noise source*. The uncertainties of thermal neutron noise obtained for the three different groups are compared in Figure 9. The neutron noise of specific group is calculated with the perturbation of parameters belonging to the considered input parameters' group, while the remaining input parameters are fixed at their nominal values. The uncertainties are obtained following 1st order Wilks' formula for two-sided limits, whose required number of code runs correspond to 93. The corresponding results are represented as follows.

The graph showing the results for the installed detector locations consists of 6 blocks along the $x-$ axis (as Figure 10), where each block corresponds to each axial position shown in Figure 4. Each block contains the values from the 6 radial detectors located in this axial position and the corresponding radial position is represented with ascending order, from position #1 (very left value in the block) to #6 (very right value in the block).

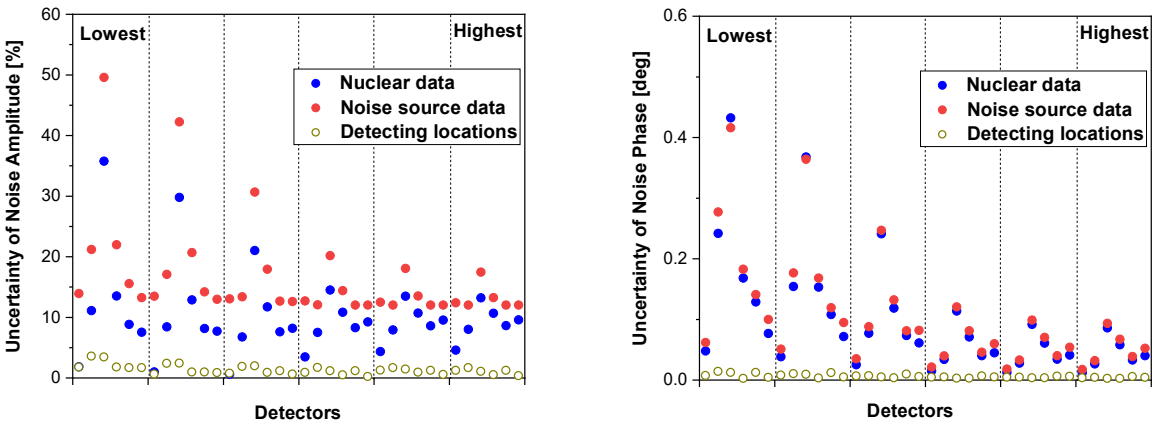

a. Amplitude of thermal neutron noise b. Phase of thermal neutron noise

Figure 9: Comparison of neutron noise uncertainties obtained from the different input parameters' groups

For both amplitude and phase of the neutron noise, the uncertainties propagated from the group of noise source data show the largest value in all detector locations, while they are followed by the uncertainties from the group of nuclear data. (The uncertainties by group of nuclear data become larger at radial position #3 at low axial positions, still, they are not remarkably different from the uncertainties from the group of noise source data.). Accordingly, the obtained result can be simply interpreted as the neutron noise being mainly driven by the group of noise source data.

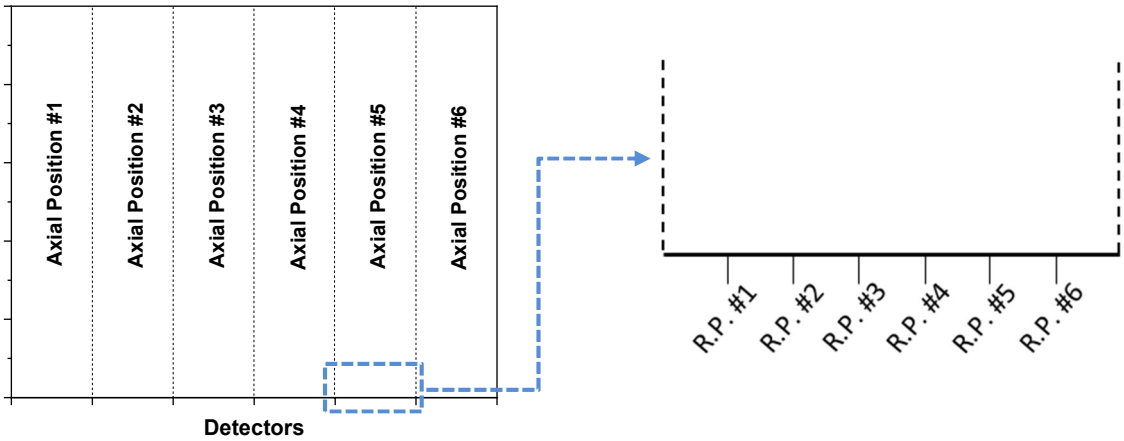

Figure 10: The composition of the graph with respect to the detector information ('R.P.' denotes 'Radial position')

Approach with Quantitative Measure

Based on the results obtained from the simplified approach, an additional analysis with quantitative measure is carried out. Here, the parameter which contributes to the neutron noise the most within the group of noise source data is quantitatively identified. This can be done by calculating the sensitivity indices for each input parameter. The calculated sensitivity indices between the three noise source data and the neutron noise are summarized in Figure 11 with 95% confidence intervals.

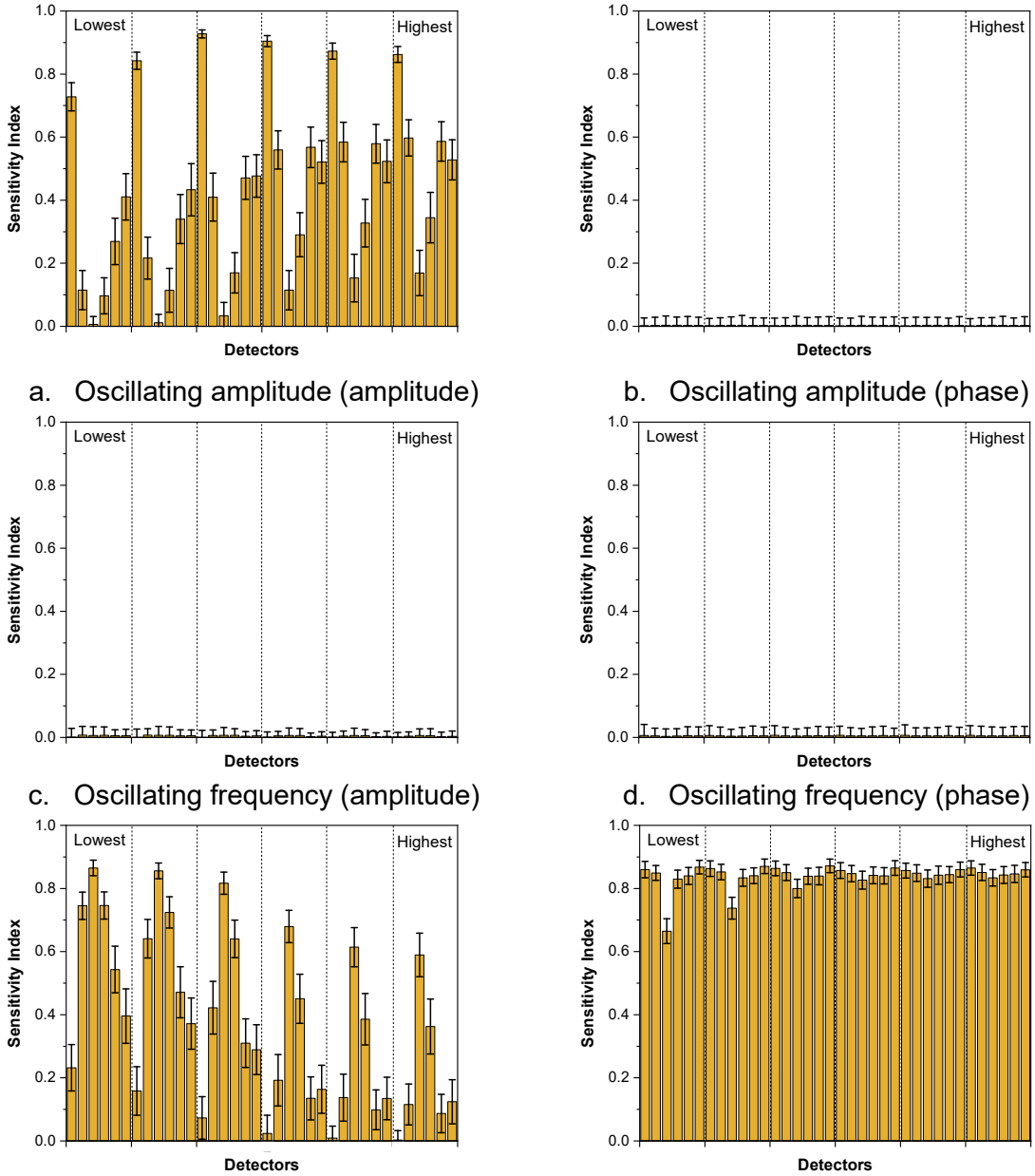

a. Oscillating amplitude (amplitude)

b. Oscillating amplitude (phase)

c. Oscillating frequency (amplitude)

d. Oscillating frequency (phase)

e. Location of noise source (amplitude)

f. Location of noise source (phase)

Figure 11: The sensitivity indices and the 95% confidence intervals between noise source data and thermal neutron noise at different detector locations

The main findings can be explained in connection with the correlation among the detector locations shown in Figure 8. For the neutron noise amplitude, the *oscillating amplitude* dominates in all axial positions at radial position #1, while the *location of the noise source* is always dominating at radial positions #3 and #4. However, at radial positions #2, #5 and #6, the *location of noise source* dominates at the lowest position and becomes weaker at higher axial positions. The decreasing effect is caught up by the increased effect of the *oscillating amplitude* and at higher axial locations, eventually, the *oscillating amplitude* becomes the main contributor.

The phase data at all detector locations are strongly dependent on the *location of noise source*, which supports the correlation information shown in Figure 8. The findings are summarized in Table 4.

Table 4: Main contributors to the neutron noise at each correlated detector locations (BOC 40)

	Correlated detectors (Number of radial position)	Main contributing parameters
Amplitude	1	Oscillating amplitude
	3, 4	Location of noise source
	2, 5, 6	Location of noise source (lower position) → oscillating amplitude (higher position)
Phase	All detectors (1~6)	Location of noise source

4.2.2 Sensitivity analysis at EOC 40

The sensitivity analysis with an identical procedure adopted in Section 4.2.1 is repeated with the core conditions of EOC 40. The different core conditions are reflected in the different values of the two-group nuclear data of the core, resulting in different noise behaviour as shown in Figure 12. The considered event (one FA oscillation) in this study brings about a larger amplitude of neutron noise at the core condition of EOC 40 than at BOC 40 (see Figure 7).

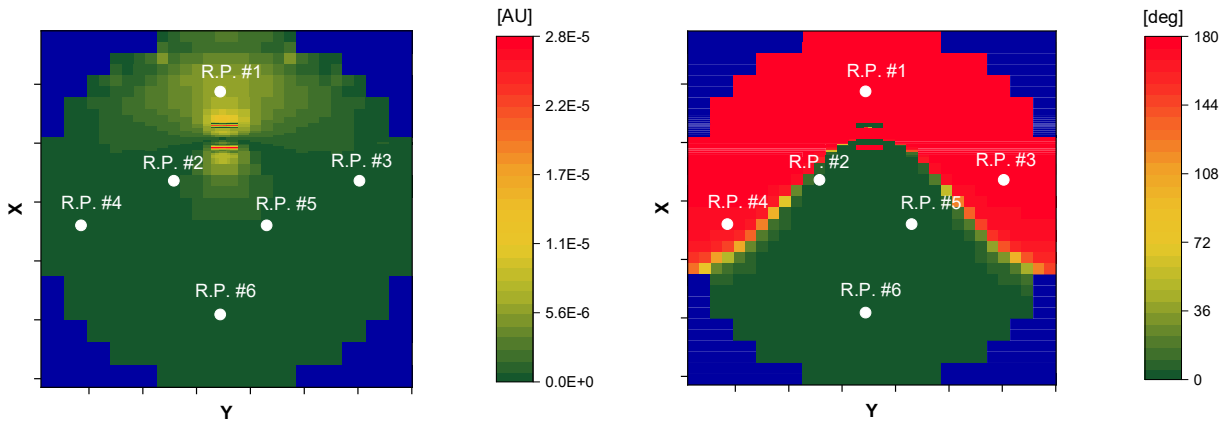

a. Amplitude b. Phase

Figure 12: Thermal neutron noise behaviour at the axial position #3 in EOC 40

<u>Analytical Issue</u>

As shown in Figure 7-b and Figure 12-b, CORE SIM+ predicts the 'out-of-phase' behaviour between two core regions around a vibrating fuel assembly. The boundary of these two regions is determined by the *location of noise source*, which is one of the input parameters considered in this study. However, the boundary reacts sensitively to the perturbation of the *noise source location*, although the perturbation corresponds to only $\pm 4.3\ mm$. The modification of the boundary can change the phase region to which the detector actually belongs, therefore, it can affect the phase signal at the installed core detectors. Figure 13 and Figure 14 show the variation of the boundary according to the perturbation of the *noise source location* at different axial positions. At the bottom position, radial positions #2, #4 and #5 can belong to two different phase regions depending on the *location of noise source*, while only radial position #4 changes regions when located at higher axial positions.

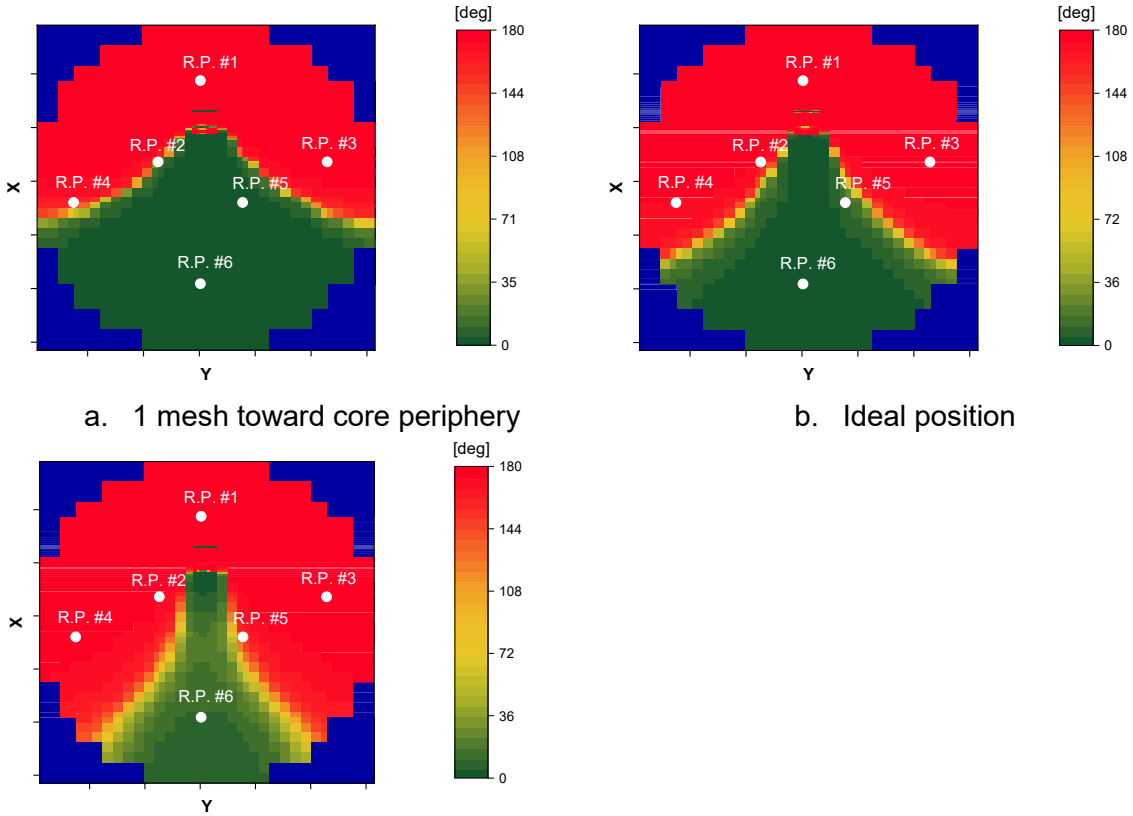

Figure 13: The phase of thermal neutron noise depending on the location of noise source (at the bottom position of the detector installation)

Consequently, when the *location of noise source* is perturbed 300 times within its uncertainty range, the obtained 300 noise solutions at these problematic detectors' locations show a discontinued distribution as shown in Figure 15. The histogram of amplitude data confirms that if a certain location may belong to two different phase regions depending on the change of the oscillating boundary, the amplitude also encounters a similar issue, which results in a discontinuity of the calculated data.

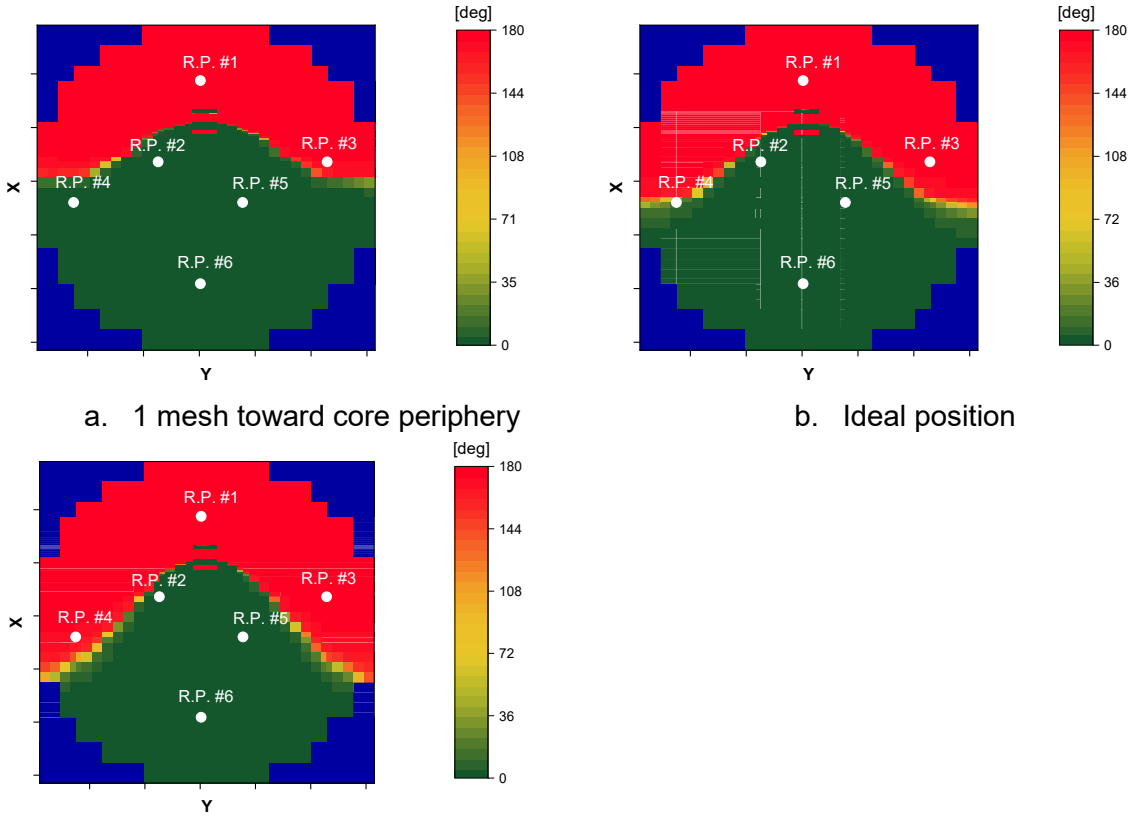

a. 1 mesh toward core periphery

b. Ideal position

c. 1 mesh toward core centre

Figure 14: The phase of thermal neutron noise depending on the location of noise source (at the mid-height position of the detector installation)

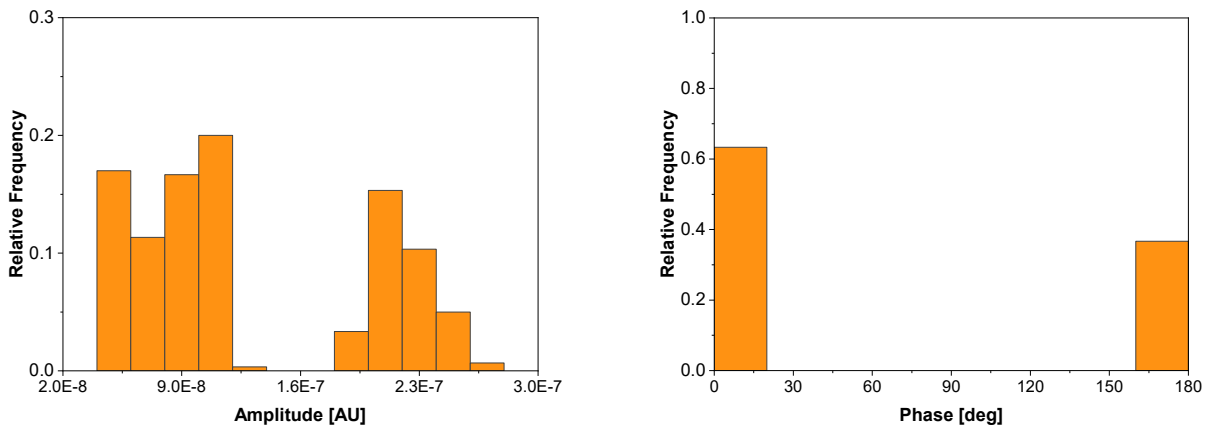

a. Amplitude

b. Phase

Figure 15: Histogram of 300 thermal neutron noise at the location of detector 4 (at the mid-height position of the detector installation)

The discontinuity existing among the calculated output data makes it impossible to adopt the regression-based approach for the further sensitivity analysis, since this approach is only valid on the premise that there is a linear relationship between the inputs and the outputs. Accordingly, the following sensitivity analysis is carried out only for the detectors which are not having this issue, namely radial positions #1, #3 and #6.

However, whether the location of a specific detector involves such a boundary issue or not is determined by the combination of two factors: the initial distribution of the nuclear data, which varies depending on the core condition, and the configuration of the in-core detectors. Therefore, the reason why all the detectors at BOC 40 are free from the aforementioned issue and valid for the

sensitivity analysis is simply a coincidence and cannot be taken as a general property of the analysed physical system.

Approach with Quantitative Measure

For the sake of conciseness, only the results of the noise source data are dealt with hereafter and discussed in connection with the results from BOC 40. The corresponding results are depicted in Figure 16. The structure of the graphs is identical to that described in Figure 9 but the data at the radial positions #2, #4 and #5 are omitted.

First of all, it should be stressed that the noise signals at the detector locations which are excluded here (radial positions #2, #4 and #5) are more sensitive to the *location of noise source* than any other input parameters. That is, despite not carrying out further statistical analysis with the data at the radial positions #2, #4, and #5, the main contributing parameter at these locations can be determined as *location of noise source* as written in Table 5.

In Figure 16 there is no remarkable change in the phase, and the *location of noise source* still maintains its dominant effect. However, different from the various correlation patterns shown at the BOC 40, the amplitude of thermal neutron noise shows monotonous dependency as summarized in Table 5: the amplitudes at radial positions #3 and #6 become strongly dependent on *the location of noise source* at all axial positions. At radial position #1, the *location of noise source* decreases its influence for higher axial locations and the decrease is caught up by the increasing influence of the *oscillating amplitude*. Nonetheless, it can be said that the contribution from the *location of noise source* is larger than at the BOC 40 (see Figure 11), in general.

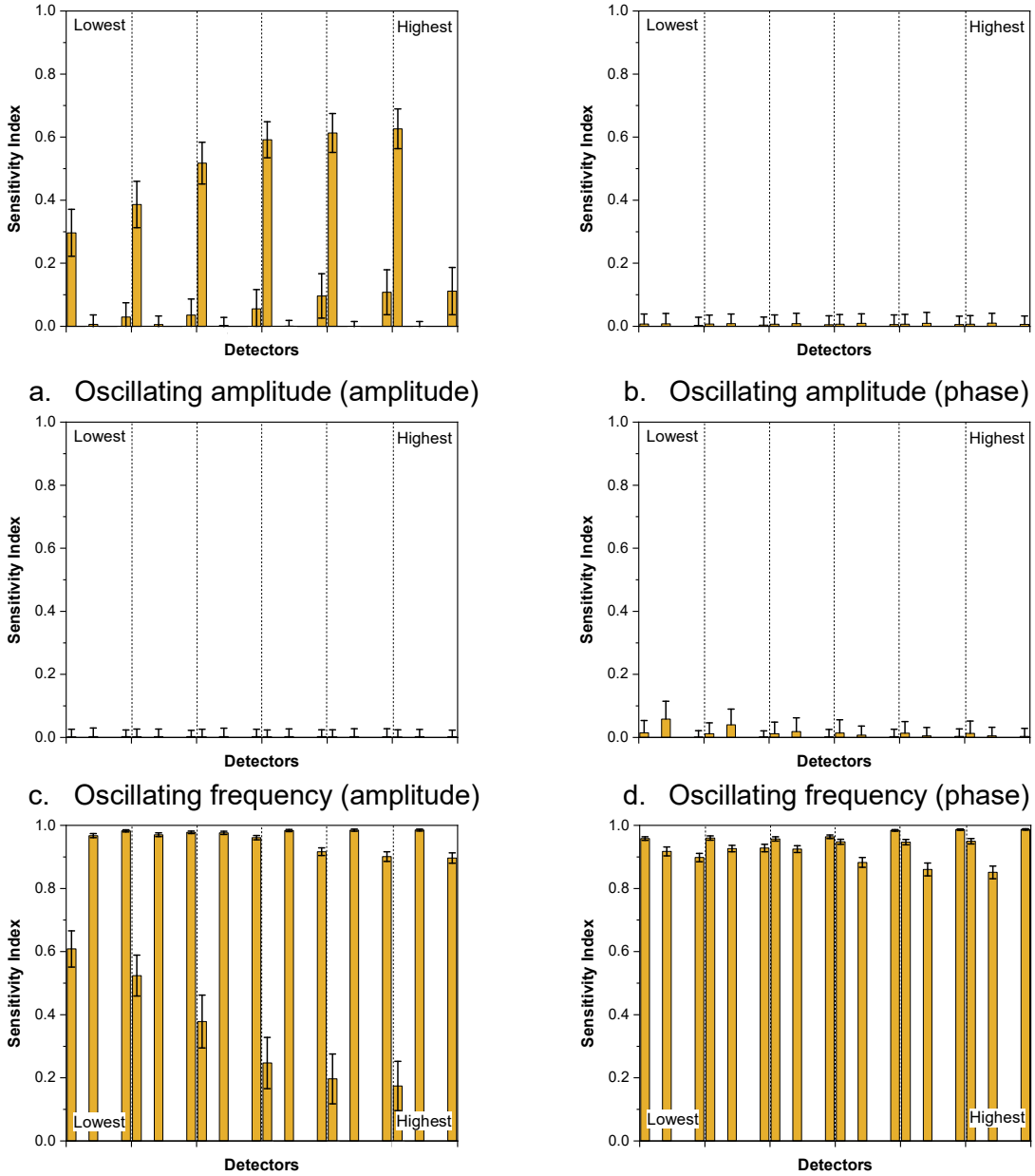

a. Oscillating amplitude (amplitude)

b. Oscillating amplitude (phase)

c. Oscillating frequency (amplitude)

d. Oscillating frequency (phase)

e. Location of noise source (amplitude)

f. Location of noise source (phase)

Figure 16: The sensitivity indices and the 95% confidence intervals between noise source data and thermal neutron noise

A reason why the *location of noise source* increases its influence remarkably at EOC 40 can be investigated in relation to the distribution of the static flux. CORE SIM+ determines the neutron noise based on two-group diffusion theory. Therefore, both the static fast and the static thermal fluxes affect the neutron noise in combination with a noise source. That is to say, even though the same magnitude of noise source is assigned to the core, the static flux can work as a weighting factor depending on the exact location of the noise source. Accordingly, the gradient of the static flux is investigated within the perturbation range of '*location of noise source*' in order to compare the 'weighting factors' between the two different core conditions: BOC and EOC.

Table 5: Main contributors to the neutron noise at the detector locations (EOC 40)

	Detectors (Number of radial position)	Main contributing parameters
Amplitude	1	Location of noise source (lower position) → oscillating amplitude (higher position)
	2~6	Location of noise source
Phase	All detectors (1~6)	Location of noise source

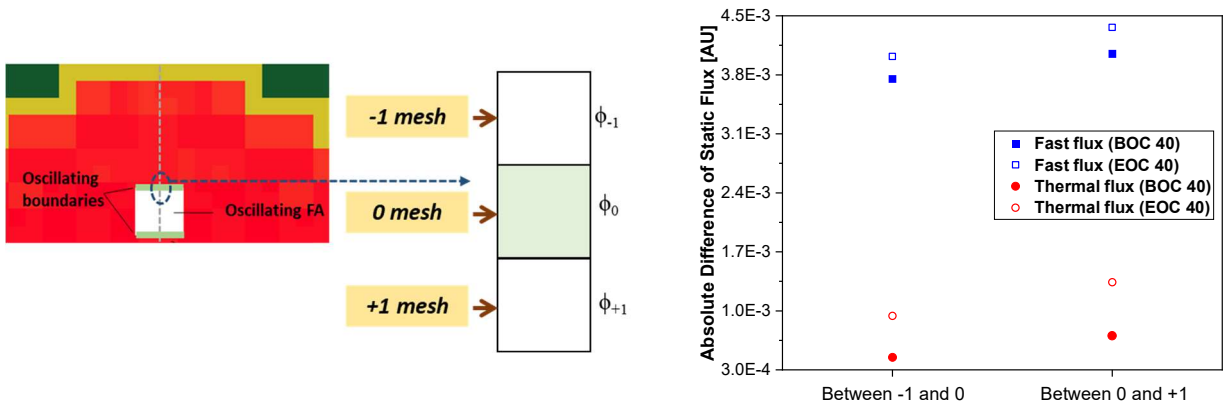

a. Oscillating boundaries perturbing between -1 and +1 meshes

b. Static flux gradients

Figure 17: The comparison of static flux gradients between BOC 40 and EOC 40

Figure 17-a shows the perturbation of the oscillating boundary in two-dimensional meshes. '0 mesh' indicates the ideal location of the oscillating boundary without perturbation, while '-1 mesh' and '+1 mesh' denote the relocation of the oscillating boundary by -1 (to the core periphery) mesh and +1 (to the core centre) mesh, respectively. Figure 17-b depicts the absolute gradient of static flux between the adjacent two meshes in Figure 17-a: between -1 mesh and 0 mesh, and between 0 mesh and +1 mesh. Both fast and thermal static fluxes at EOC 40 have steeper gradients around the oscillating boundaries than at BOC 40. Consequently, the noise source at the oscillating boundaries at EOC 40 is weighted more than at BOC 40 when the assigned location is perturbed, which justifies the increased influence of '*location of noise source*' on the neutron noise.

4.2.3 Sensitivity analysis at EOC 39

Figure 18 shows the distribution of the thermal neutron noise in the radial core direction under unperturbed conditions.

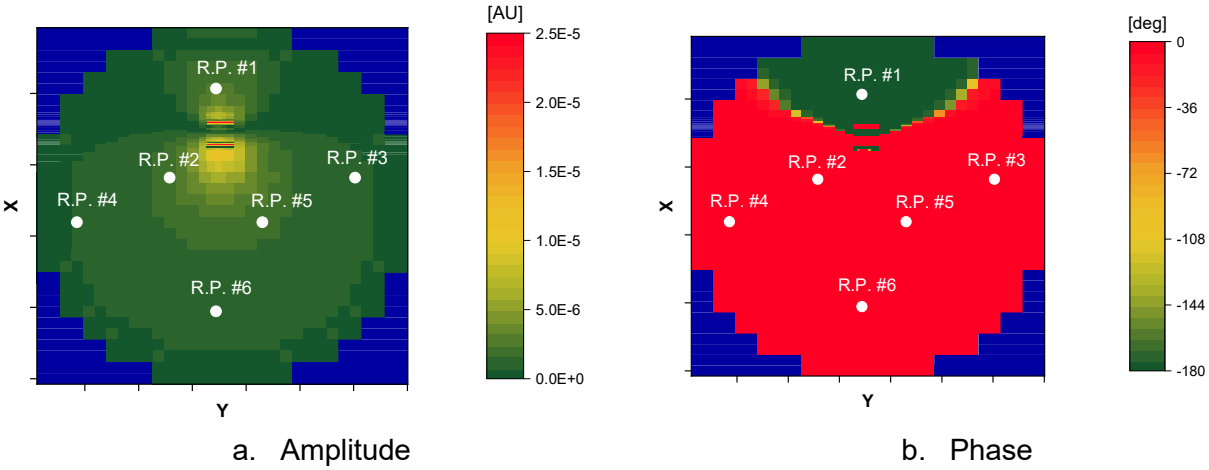

a. Amplitude b. Phase

Figure 18: Thermal neutron noise behaviour at the axial position #3 in EOC 39

Analytical Issue

The identical issue reported at EOC 40 is also found at EOC 39 with different pattern as shown in Figure 19. The problematic point is found at the radial position #1 between the mid-height and the top of the core. Therefore, the following sensitivity analysis is carried out for all detectors except for those at radial position #1.

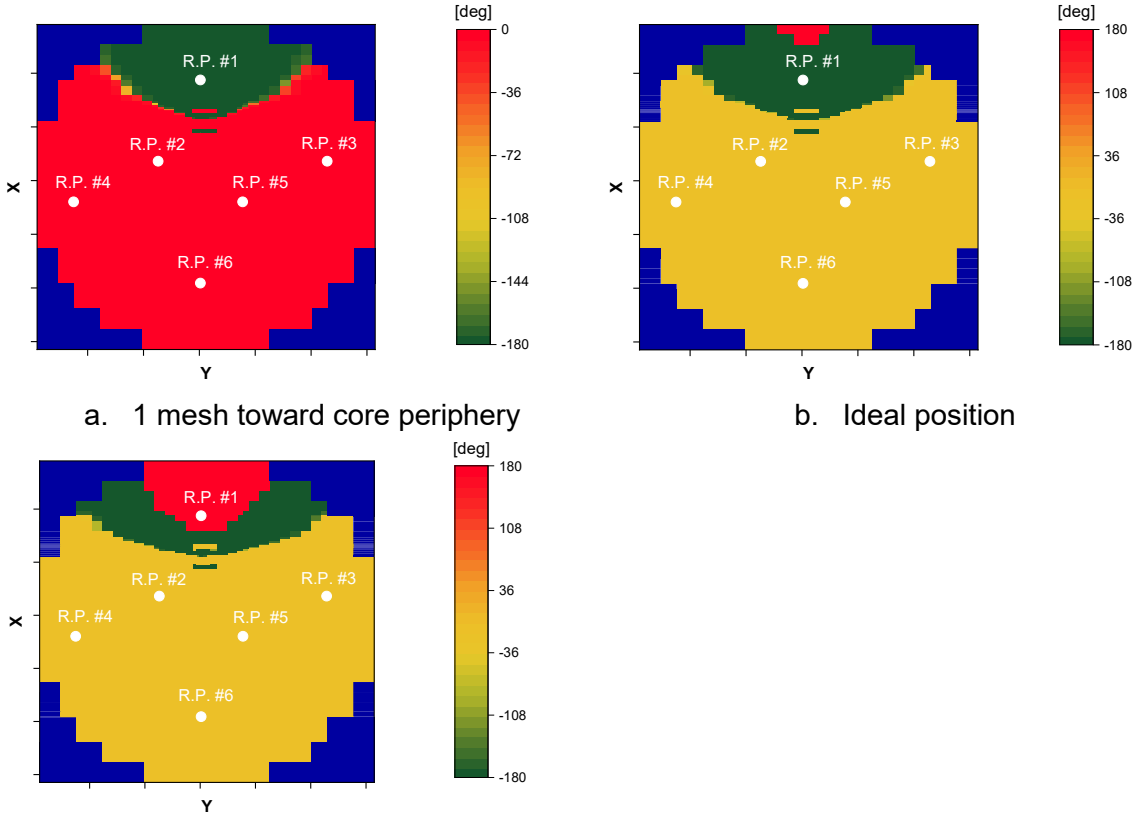

a. 1 mesh toward core periphery b. Ideal position

c. 1 mesh toward core centre

Figure 19: The phase of thermal neutron noise depending on a location of noise source (at the mid-height position of the detector installation)

Approach with Quantitative Measure

Figure 20 summarizes the sensitivity indices of the noise source data at the installed detector locations, except for radial position #1 at all axial levels.

The results at EOC 39 are more easily to explain compared to the previous results under different core conditions (see Table 7), since all detector locations show a relatively similar pattern.

The *oscillating amplitude* affects the amplitude of the noise in a significant manner. Nonetheless, still the *location of noise source* shows the largest influence and maintains its position as a most influential parameter for all axial positions. In the case of the phase, the *oscillating frequency* shows a visible influence, which decreases as the detecting position gets higher axially. However, the *location of noise source* has a dominant effect and overwhelms the influence from the *oscillating frequency*.

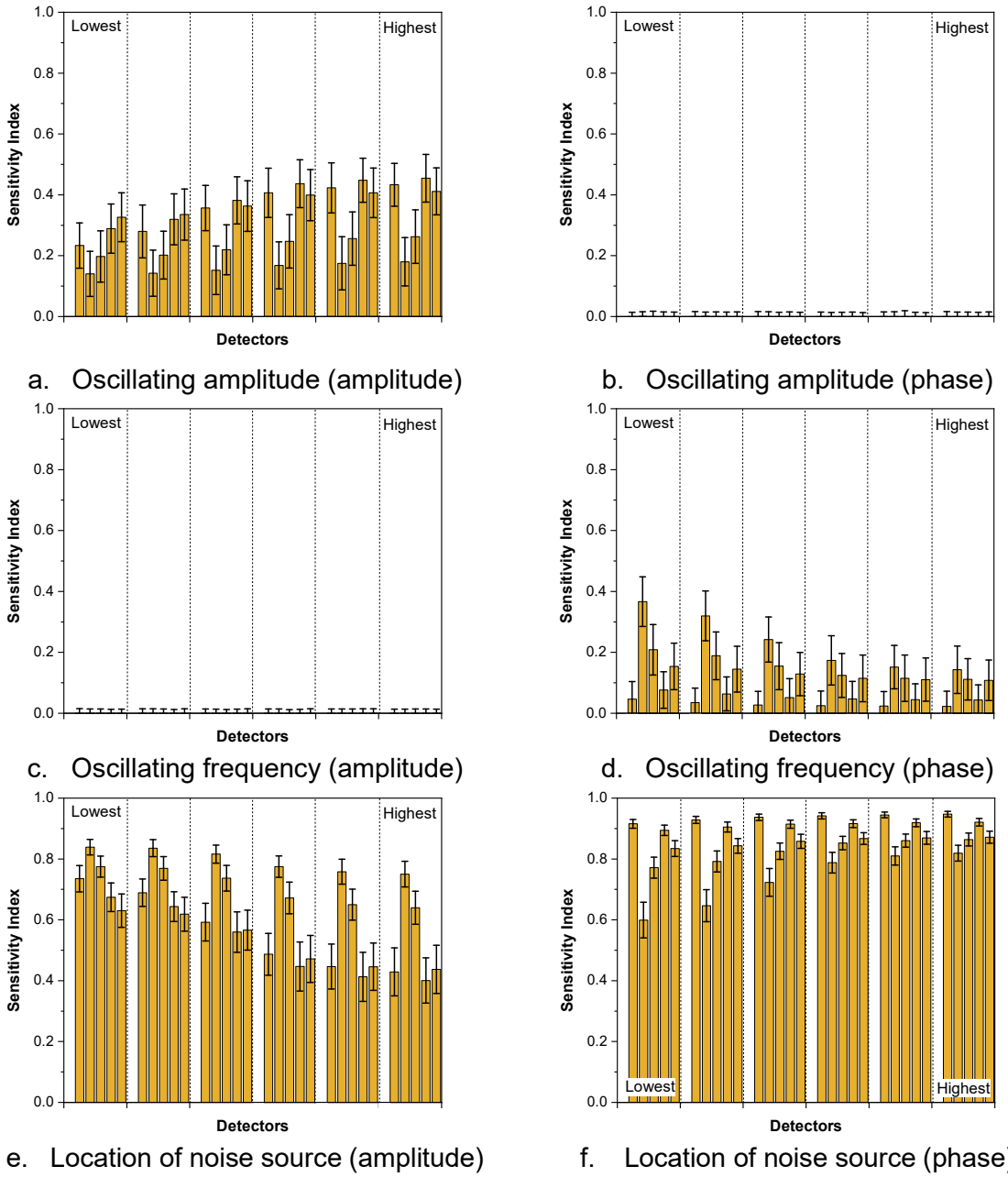

Figure 20: The sensitivity indices and the 95% confidence intervals between noise source data and thermal neutron noise

Table 6: Main contributors to the neutron noise at the detector locations (EOC 39)

	Detectors (Number of radial position)	Main contributing parameters
Amplitude	All detectors (1~6)	Location of noise source
Phase	All detectors (1~6)	Location of noise source

5 Conclusions

The obtained results from the sensitivity analyses in three different core conditions can be summarized as Table 7.

The main findings can be explained in relation to the effects of the fuel burnup and fuel loading pattern. The phase of the neutron noise is strongly driven by the *location of noise source* regardless of the burnup condition and of the fuel loading pattern. The amplitude, however, shows various dependencies depending on the radial and axial position of interest. At the BOC 40, the *oscillating amplitude* shows a remarkable influence at some detector locations and competes with the *location of noise source* for the more influential parameter. At the EOC 40, however, owing to the steeper gradients of the static fluxes at the oscillating boundaries, the *location of noise source* increases its influence, and the *oscillating amplitude* contributes less than it does at the BOC 40.

The changes of fuel loading pattern result in minor differences in the results. At the EOC 39, no strong competition among the parameters is found but the *location of noise source* maintains its dominant effect in all detector locations.

It should be pointed out that the sensitivity of the induced neutron noise on the noise source (location and amplitude) is one of the main reasons why the machine learning-based unfolding techniques developed in CORTEX works satisfactorily. Any change related to the noise source results in significant changes in the response of the reactor, which are thus “detected” by the machine learning algorithms. This allows differentiating the type of noise source existing in the core, as well as its possible location.

The analysis of the dependence of the noise pattern within the fuel cycle and between the fuel cycles also tends to indicate that the spatial pattern of the induced neutron noise has a rather significant dependence on burnup and core loading.

Table 7: Main contributors to the neutron noise under the different core conditions

	Amplitude		Phase	
	Detectors (Number of radial position)	Main contributing parameters	Detectors (Number of radial position)	Main contributing parameters
BOC 40	1	Oscillating amplitude	All detectors (1 ~ 6)	Location of noise source
	3, 4	Location of noise source		
	2, 5, 6	Location of noise source (lower position) → oscillating amplitude (higher position)		
EOC 40	1	Location of noise source (lower position) → oscillating amplitude (higher position)	All detectors (1 ~ 6)	Location of noise source
	2 ~ 6	Location of noise source		
EOC 39	All detectors (1 ~ 6)	Location of noise source	All detectors (1 ~ 6)	Location of noise source

6 References

[1] Kernkraftwerk Gösgen-Däniken AG (KKG), Technical Brochure 'Technology and Operation,' (2016). URL https://www.kkg.ch/upload/cms/user/KKG_TB_englisch_2016.pdf

[2] Gösgen, CORTEX Internal Technical Report, Gösgen Contribution to D 4.2 (2018).

[3] Technical University of Dresden, "Training Reactor AKR-2: Technical Description and Procedure of Operation for the Reactor Facility AKR-2," (2015).

[4] V. Lamirand, M. Hursin, P. Frajtag and A. Pautz, "Future Experimental Programmes in the CROCUS Reactor," RRFM/IGORR 2016, Berlin, Germany, March 13-17 (2016).

[5] C. Demazière et al. "Description of scenarios for the simulated data," Technical Report D3.1 (2019). URL http://cortex-h2020.eu/wp-content/uploads/2019/07/CORTEX_D3_1_Description_of_scenarios_for_the_simulated_data_V1.pdf

[6] A. Mylonakis et al., "CORE SIM+: A flexible diffusion-based solver for neutron noise simulations," Annals of Nuclear Energy, **155**, 108149 (2021).

[7] C. Demazière, "CORE SIM: A multi-purpose neutronic tool for research and education," Annals of Nuclear Energy, **38**, pp.2698-2718 (2011).

[8] S. Yum et al., "Methodology for uncertainty and sensitivity analysis," Technical Report D1.1 (2019). URL http://cortex-h2020.eu/wp-content/uploads/2019/07/CORTEX_D1_1_Methodology_for_uncertainty_and_sensitivity_analysis_V1.pdf

[9] Gösgen, "Data compilation - Gösgen core cycles 39 & 40 – CORTEX," BER-F-92430, Version 1 (2018).

[10] B. T. Rearden and M. A. Jessee, "SCALE Code System, ORNL/TM-2005/39, Version 6.2.1," Oak Ridge National Laboratory, Oak Ridge, TN (2016).

[11] C. Demazière, "Description of the models and algorithms used in the CORE SIM neutronic tool," Chalmers University of Technology, CTH-NT-241 (2011).

[12] W. J. Conover, "Practical Nonparametric Statistics," 3rd ed., John wiley & Sons, New York (1980).

[13] SPSS Tutorials: Pearson Correlation, URL: https://libguides.library.kent.edu/SPSS

[14] P. H. Ramsey, "Critical Values for Spearman's Rank Order Correlation," Journal of Educational Statistics, **14(3)**, pp.245-253 (1989).

[15] S. Kajuri, "Application of Hypothesis Testing and Spearman's rank correlation coefficient to demystify Suicides worldwide," (2018) URL https://towardsdatascience.com/application-of-hypothesis-testing-and-spearmans-rank-correlation-coefficient-to-demystify-b3a554730c91

[16] A. G. Bluman, "Elementary Statistics: A Brief Version," 7th Edition, New York: McGraw-Hill (2009).

[17] F. Sarrazin, F. Pianosi and T. Wagener, "Global Sensitivity Analysis of environmental models: Convergence and Validation," Environmental Modelling & Software, **79**, pp.135-52 (2016).